Cerebral Cortex November 2013;23:2690–2699
doi:10.1093/cercor/bhs257
Advance Access publication August 23, 2012

Differential Wiring of Layer 2/3 Neurons Drives Sparse and Reliable Firing During Neocortical Development

Brett L. Benedetti[1,2,†], Yoshio Takashima[1,†], Jing A. Wen[1], Joanna Urban-Ciecko[1] and Alison L. Barth[1]

[1]Department of Biological Sciences and Center for the Neural Basis of Cognition, Carnegie Mellon University, Pittsburgh, PA, USA, [2]Present address: NYU Neuroscience Institute, Department of Physiology and Neuroscience, Smilow Research Center, New York University School of Medicine, 522 First Avenue, New York, NY 10016, USA.

Address correspondence to Alison L. Barth, Department of Biological Sciences and Center for the Neural Basis of Cognition, Carnegie Mellon University, 4400 Fifth Avenue, Pittsburgh, PA 15213, USA. Email: barth@cmu.edu
[†]These authors contributed equally to this work.

Sensory information is transmitted with high fidelity across multiple synapses until it reaches the neocortex. There, individual neurons exhibit enormous variability in responses. The source of this diversity in output has been debated. Using transgenic mice expressing the green fluorescent protein coupled to the activity-dependent gene *c-fos*, we identified neurons with a history of elevated activity in vivo. Focusing on layer 4 to layer 2/3 connections, a site of strong excitatory drive at an initial stage of cortical processing, we find that fluorescently tagged neurons receive significantly greater excitatory and reduced inhibitory input compared with neighboring, unlabeled cells. Differential wiring of layer 2/3 neurons arises early in development and requires sensory input to be established. Stronger connection strength is not associated with evidence for recent synaptic plasticity, suggesting that these more active ensembles may not be generated over short time scales. Paired recordings show fosGFP+ neurons spike at lower stimulus thresholds than neighboring, fosGFP− neurons. These data indicate that differences in circuit construction can underlie response heterogeneity amongst neocortical neurons.

Keywords: AMPA receptors, activity-dependent gene expression, critical period, somatosensory, subnetworks

Introduction

Sensory stimulation drives reliable firing of peripheral and subcortical neurons, where every stimulus can trigger a spike in a given cell. In contrast, the response properties of cortical neurons exhibit enormous variability, with some cells firing significantly more than others (Brecht et al. 2003; Ohki et al. 2005; de Kock et al. 2007; Kerr et al. 2007; Hromadka et al. 2008; Poo and Isaacson 2009; Stettler and Axel 2009; Wolfe et al. 2010; Barth and Poulet 2012). The source of firing variability across different cells has been debated. Response heterogeneity might reflect differences in the intrinsic electrophysiological properties of neurons (Marder and Goaillard 2006; Padmanabhan and Urban 2010), or arise from differences in synaptic input to a subset of cells (MacLean et al. 2005; Yoshimura et al. 2005). Alternatively, because the majority of studies have serially sampled neurons over short periods of time, differences in firing output might arise from fluctuations in cortical state or background activity (Arieli et al. 1996; Petersen et al. 2003) or the presence of neuromodulators that transiently influence firing (Metherate et al. 1992; Steriade et al. 1993; Constantinople and Bruno 2011). Understanding why neocortical neurons show such diverse response properties will require the systematic analysis of specific cells and circuits in this brain area.

In order to identify candidate neurons that might show higher sensory-evoked activity and to determine the mechanistic basis for this difference, we targeted neurons that expressed the green fluorescent protein (GFP) under the control of the activity-dependent gene *c-fos* for electrophysiological recording (Barth et al. 2004). *C-fos* is expressed by ~15% of layer 2/3 neurons in primary somatosensory cortex under basal, unstimulated conditions (Yassin et al. 2010). Previous studies have shown that this immediate-early gene (IEG) can be driven by synaptic activity and neural firing (Sheng et al. 1990; Schilling et al. 1991; Luckman et al. 1994; Fields et al. 1997; Schoenenberger et al. 2009) but see Guzowski et al. (2006); since expression here was activated by the animal's normal experience in vivo, it is not clear what specific stimulus was responsible for fosGFP induction.

Previous studies have shown that basal IEG expression in layer 2/3 neurons is correlated with elevated spontaneous firing activity, both in vivo and in vitro (Yassin et al. 2010). It might originate from spontaneous cortical activity; alternatively, it might be specifically related to sensory input from the periphery. These two possibilities are not mutually exclusive, as there is a strong overlap between the circuits activated by sensory input and spontaneous activity (Kenet et al. 2003; MacLean et al. 2005; Marre et al. 2009).

Here, we test the hypothesis that a subset of layer 2/3 neurons exhibiting IEG expression receives stronger excitatory drive from layer 4, the input layer of the cortex. Paired-cell voltage-clamp recordings showed that fosGFP+ neurons received a 2-fold increase in glutamatergic synaptic strength compared with fosGFP− neurons. This difference in input strength required sensory input to be established but not maintained. Paired-cell current-clamp recordings showed that fosGFP+ neurons fired at reduced layer 4 stimulation intensities compared with neighboring, unlabeled cells. These data show that a subset of layer 2/3 neurons marked by IEG expression may dominate firing output under some stimulation conditions, and that response heterogeneity in the neocortex may be at least partly attributed to the differential wiring of layer 2/3 neurons within the neocortical circuit.

Materials and Methods

Brain Slice Preparation

Brain slices containing primary somatosensory cortex were prepared from unstimulated mice P9–P22 (fosGFP heterozygous or arcGFP heterozygous animals), removed from their home cage where they were group housed. The broad age range was used to examine the

developmental regulation of inputs to layer 2/3 neurons; unless indicated, slices were prepared from animals P12–16. Within 10–15 min of removal from their home cage, mice were briefly anaesthetized with isoflurane and decapitated. Coronal brain slices (350 μm thick) containing primary somatosensory cortex were cut in chilled artificial cerebral spinal fluid (ACSF) composed of (in mM): 119 NaCl, 2.5 KCl, 1.3 $MgSO_4$, 2.5 $CaCl_2$, 1 NaH_2PO_4, 26 $NaHCO_3$, 11 glucose, ~295 mOsm, equilibrated with 95/5% O_2/CO_2. Slices were allowed to recover for 1 h before recording. Recovery and recordings were carried out at room temperature.

Evoked Synaptic Responses

For whole-cell voltage-clamp recordings, internal electrode solution was composed of (in mM): 130 cesium gluconate, 2.8 NaCl, 10 4-(2-hydroxyethyl)-1-piperazineethanesulfonic acid (HEPES), 0.5 ethylene glycol tetraacetic acid, 5 tetraethyl ammonium chloride, 4 Mg-ATP, 0.4 Na-GTP, pH 7.2–7.3, ~290 mOsm. Layer 2/3 fosGFP+ and fosGFP− neurons in the center of the barrel column were identified on the basis of their intrinsic GFP expression and subsequently targeted for whole-cell recording. Upon achieving the whole-cell configuration in a pair of neurons, responses were evoked by extracellular stimulation in layer 4 at a frequency of 0.1 Hz. Note that use of the term "pair" does not indicate that the 2 neurons that were simultaneously recorded were synaptically connected. A glass monopolar stimulating electrode (tip diameter ~50 μm) filled with ACSF was placed in the center of a layer 4 barrel just below the site of layer 2/3 recording. Neurons for dual-cell recordings were located within the same barrel column. To remove the possibility of prolonged stimulation altering experimental outcomes via plasticity induction, the stimulus electrode was moved to a new barrel column, or to a new slice after successfully recording from a pair of neurons.

To isolate excitatory post-synaptic currents (EPSCs), neurons were maintained at −70 mV and responses were collected in the presence of the gamma-aminobutyric acid-receptor antagonist picrotoxin (50 μM). Layer 4 stimulation intensity was gradually increased until a short-latency (3–6 ms) EPSC was observed in both neurons. Instances in which one or both of the neurons failed to respond were not included in analysis, and subsequently another pair was attempted. For most pairs in which reliable responses could be evoked, EPSCs were then collected at multiple stimulation intensities in order to sample a range of response amplitudes typically ranging between 20 and 200 pA. Ten to 20 stimulation trials were collected at each intensity and used for analysis. To directly compare EPSCs recorded in different pairs and from different slice preparations, we analyzed evoked responses from trials taken at the minimum stimulation intensity capable of generating a reliable response >20 pA and <175 pA in both neurons.

Paired-pulse ratios (PPRs) of EPSC amplitudes were calculated using 2 stimulus pulses separated by 50 ms, where the amplitude of the second pulse was divided by that of the first. PPRs were determined from both paired and single-cell recordings. Typically one 50 ms paired-pulse interval was tested (with only two stimuli), and the response was averaged over a small number of trials (~10 per cell). A short (500 ms) test pulse at the beginning of each trial was used to monitor series and input resistances throughout the recording and only cells with a stable input resistance > 100 MΩ and series resistance < 50 MΩ were included for analysis.

Sr-Excitatory Post-synaptic Currents Collection and Analysis

To isolate quantal 2-amino-3-(5-methyl-3-oxo-1,2-oxazol-4-yl)propanoic acid receptor-mediated EPSCs, (2R)-amino-5-phosphonovaleric acid; (2R)-amino-5-phosphonopentanoate (D-APV) (50 μM) and picrotoxin (50 μM) were included in the bath solution that contained ACSF with 1 mM $MgSO_4$ and 3 mM Sr^{2+} instead of Ca^{2+} in order to drive asynchronous glutamate release. Neurons were voltage-clamped at −70 mV and 5 mM QX-314 (lidocaine *N*-ethyl bromide) a Na+ channel antagonist, was included in the internal solution to reduce noise. The evoked response has an initial synchronous component (~50 ms after the stimulus artifact) that was excluded in the analysis. Isolated, asynchronous events that occurred from 50 to 500 ms after the stimulus were manually selected and analyzed using Minianalysis software (Synaptosoft). Event threshold was set at 2× root mean square noise (usually about 4–5 pA), and data were low-pass filtered at 1 kHz. Recordings for Sr-EPSCs were conducted using single-cell (not dual-cell) recordings. Approximately 100 random events were selected for each cell and grouped for comparison. Traces for each cell were first averaged, and then these traces were averaged across cells in a group to yield a group mean.

Juxta-Cellular and Whole-Cell Current Clamp Recordings

For juxta-cellular and whole-cell recordings, the internal solution contained in mM: K-gluconate 100, KCl 20, HEPES 10, Mg-ATP 4, Na-GTP 3, pH 7.4, 280–290 mOsm. For juxta-cellular recordings, cell soma with a pyramidal morphology were targeted. In whole-cell recordings, pyramidal morphology and the presence of dendritic spines were confirmed upon filling with the dye Alexa-568.

Evoked Firing

No drugs were included in the bath solution unless indicated in the text. For each pair, stimulus intensity applied to layer 4 was adjusted to sample a range of spiking response probabilities (typically 5–8 intensities per pair), such that a response probability of 1 was observed in at least one of the neurons (preferably in both neurons). Ten to 20 trials at 0.1 Hz were collected at each stimulus intensity. Spike times between 3 and 30 ms post-stimulus were identified using a custom-written Igor macro to detect AP peak. Spikes at shorter latencies than 3 ms resulted from antidromic stimulation of layer 3 neurons, and were not included in analysis. Typically, evoked spikes did not occur after the first 15 ms post-stimulus and little recurrent activity was observed. Stimulus–response curves of response probability were generated for each pair, calculated as the fraction of trials at each stimulus intensity where a spike was evoked. To analyze spike latency and precision from different recordings, these measurements were taken from the lowest stimulation intensity that generated the most reliable response (typically 100% or a short latency spike for all trials) in at least one of the recorded neurons. Stimulus intensity at 50% of firing probability was determined by applying Boltzmann fit to the response probability curve (Origin software).

Evoked Inhibitory Post-synaptic Currents

To record layer 4-evoked IPSCs, neurons were voltage-clamped at +10 mV. Monosynaptic IPSCs were evoked by layer 4 stimulation in the presence of D-APV (50 μM) and 2,3-dihydroxy-6-nitro-7-sulfamoyl-benzo[f]quinoxaline-2,3-dione (NBQX) (5 μM). For both mono- and polysynaptic IPSCs, amplitude values for a given pair were included in the dataset if they fell within the range 25–300 pA. Response latencies for polysynaptic IPSCs were more variable than for EPSCs, and also changed sharply with stimulus intensity, likely due to the scattered distribution of inhibitory neurons in the vicinity of the recording electrode. Ten to 20 stimulation trials were averaged at multiple stimulus intensities for each recorded pair of neurons.

Statistical Analysis

For paired recordings, comparisons between GFP+ and GFP− neurons (in fosGFP or arcGFP transgenic mice) were performed using paired *t*-tests. For datasets comprised of single-cell recordings, GFP+ and GFP− neurons were compared using the non-parametric Mann–Whitney *U* test (unpaired). All data are displayed as mean ± standard error of the mean (SEM) unless indicated.

Results

Difference in Excitatory Synaptic Drive Onto fosGFP+ and fosGFP− Neurons

To test whether neurons exhibiting elevated spontaneous activity received stronger excitatory drive from layer 4 stimulation, acute brain slices were prepared from unstimulated

fosGFP transgenic mice in 2–3-week-old animals. Under these conditions, ~15% of layer 2/3 neurons exhibit fosimmunoreactivity or express the fosGFP transgene (Yassin et al. 2010). Since transgene expression is not induced by brain slice preparation (Barth et al. 2004), GFP fluorescence serves as a reporter of prior events that occurred in vivo.

An extracellular stimulating electrode was placed in layer 4, and pairs of fosGFP+ and fosGFP− neurons were targeted for dual whole-cell recordings in lower layer 2/3 (Fig. 1*A* and Supplementary Figure S1; fosGFP+ 292 ± 7 μm vs fosGFP− 286 ± 9 μm from pial surface, $n = 17$). Pharmacologically isolated, short-latency (~3–6 ms; see also Supplementary Fig. S1) EPSCs were recorded following layer 4 stimulation, and the amplitude of these responses was compared across trials and multiple stimulus intensities for fosGFP+ and fosGFP− pairs (Fig. 1*B–C*). For EPSC measurements, dual-cell recordings were critical, since small differences in the angle of the acute brain slice or the health of the tissue could result in large slice-to-slice variation in response amplitudes and make small differences difficult to detect. However, these potential confounds are eliminated when all comparisons are done between simultaneously recorded cells.

We observed that fosGFP+ neurons showed EPSCs that were significantly larger both within a trial and on average compared with simultaneously recorded fosGFP− cells (Fig. 1*D,F*; fosGFP+ 64.5 ± 10.6 pA vs fosGFP− 36.5 ± 4.2 pA, $n = 17$, $P < 0.05$). This was the case across multiple stimulation intensities for each pair (Supplementary Fig. S2). Other recording parameters, such as series resistance and onset latency were comparable between cell types, although input resistance was higher in fosGFP+ neurons at this age (Supplementary Fig. S1).

These findings were also observed in another transgenic reporter of neural activity. ArcGFP animals are BAC transgenic mice that carry GFP knocked-in to the endogenous *arc* locus (generated through the GENSAT project; http://www.gensat.org/index.html), and GFP expression is thought to mirror expression of the endogenous *arc* gene. Importantly, GFP expression in this transgenic line is not localized to the nucleus, reducing concerns about a potential effect of the fosGFP transgene. Dual-cell recordings from animals aged P12–16 indicate that arcGFP+ cells have an approximately 2-fold larger EPSC compared with arcGFP− cells (Fig. 1*E,F*; arcGFP+ 68.3 ± 12.6 pA vs 38.3 ± 4.9 pA, $n = 6$, $P < 0.05$). In this smaller dataset, we noted that input resistance was lower in arcGFP+ cells, suggesting that differences in this property are not sufficient to explain larger EPSC amplitudes across both types of IEG transgenics.

Taken together, the difference in input strength cannot be attributed to a specific property of the transgenic line used or expression of the fluorescent reporter in the post-synaptic cell. Rather, these data indicate that expression of activity-dependent IEGs is associated with strong synaptic drive from layer 4 stimulation during postnatal development.

Input Number, not Input Amplitude, is Larger for fosGFP+ Neurons

Stronger excitatory drive to layer 2/3 neurons might arise from an increased number of inputs, an increased probability of

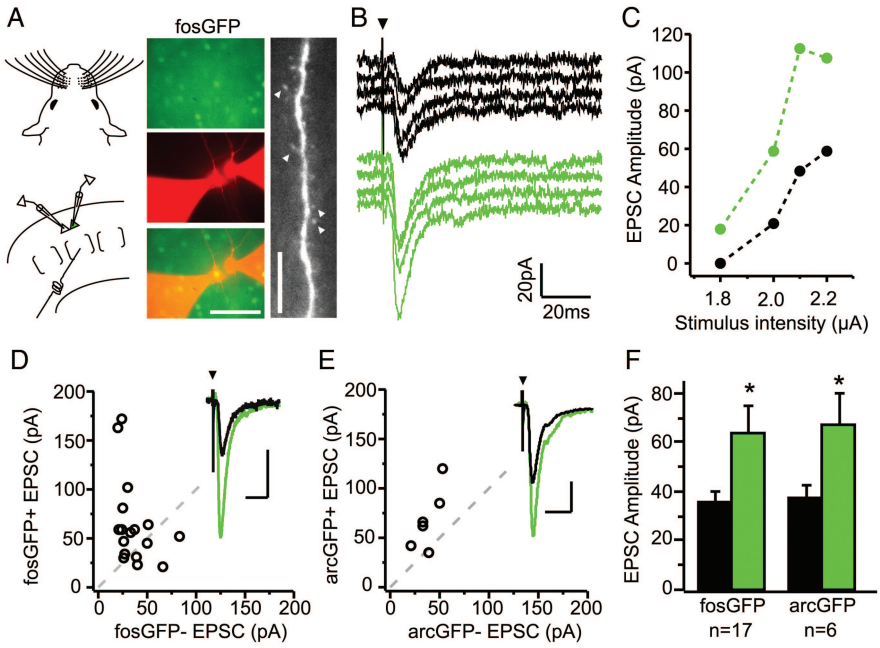

Figure 1. Excitatory synaptic drive is stronger onto fosGFP+ neurons. (*A*) Experimental configuration for dual whole-cell recordings in acute brain slices from unstimulated, cage-reared fosGFP mice (left). FosGFP expression used to target whole-cell patch pipettes to fosGFP+ and fosGFP− pyramidal neurons (middle). Scale bar, 50 μm. Apical dendrite of a recorded neuron filled with Alexa-568 to reveal the presence of dendritic spines (arrowheads; right). Scale bar, 10 μm. (*B*) Example responses evoked by layer 4 (L4) stimulation (4 trials, 0.1 Hz) recorded simultaneously in a fosGFP− (black) and fosGFP+ (green) neuron. Arrowhead indicates stimulus onset. Stimulus artifact has been truncated for clarity. (*C*) Stimulus response curve of excitatory synaptic strength in one pair of L2/3 neurons evoked by increasing stimulus strength in L4. (*D*) Scatter plot comparison of mean EPSC amplitudes recorded from 17 fosGFP+/− pairs between P12–14. Dashed line indicates unity. Inset shows the example average EPSC from one pair, scale bars, 40 pA, 20 ms. (*E*) Scatter plot comparison of EPSC amplitudes recorded from 6 arcGFP+/− pairs. Inset shows example average EPSC from one pair, scale bars, 20 pA, 20 ms. (*F*) Mean ± SEM evoked EPSC amplitudes for fosGFP+/− and arcGFP pairs+/−. Asterisk indicates $P < 0.05$.

release at presynaptic contacts onto fosGFP+ neurons, a stronger post-synaptic response, or some combination of these factors. Answers to these questions would, in turn, help elucidate the mechanisms that underlie the establishment of these highly active subnetworks—specifically, whether these differences arise during normal development or are assembled via activity-dependent plasticity mechanisms.

To examine whether the quantal amplitude, or the size of the post-synaptic response to a single vesicle release event, was different between the two groups of cells, we used an extracellular solution where Ca^{2+} had been replaced with Sr^{2+} to promote asynchronous vesicle release (Goda and Stevens 1994; Xu-Friedman and Regehr 1999; Thomas et al. 2001). This method allows analysis of a pathway-specific post-synaptic response for individual contacts onto a given cell, a function that should be consistent across preparations. Accordingly, paired-cell recordings were not required for these measurements.

Mean Sr-EPSC amplitude is determined from the average of 50–100 or more individual events. Because previous studies from our laboratory have demonstrated that altered sensory experience can potentiate Sr-EPSC amplitude by 15–20% (Clem and Barth 2006; Clem et al. 2008; Wen and Barth 2011), we were confident that this method is sensitive enough to detect small changes in input amplitude if they are present. These recordings revealed that the mean amplitude of the Sr-EPSC, averaged over ~100 events per cell, for layer 2/3 fosGFP+ neurons was not significantly different than nearby fosGFP− neurons (Fig. 2*A–C*; fosGFP+ 10.10 ± 0.42 pA, $n = 17$ vs fosGFP− 10.98 ± 0.61 pA, $n = 14$).

Differences in the amplitude of the multiquantal EPSC response could result from an increased presynaptic release probability of layer 4 inputs onto fosGFP+ neurons; however, analysis of the PPR did not support this interpretation. The PPR was facilitating for layer 2/3 neurons at this developmental stage, and was similar for the two cell populations (Fig. 2*D–E*; PPR fosGFP+ 1.37 ± 0.08, $n = 11$ vs PPR fosGFP− 1.51 ± 0.17, $n = 12$). Thus, increased probability of release for layer 4 inputs onto fosGFP+ neurons is not an adequate explanation for the stronger excitatory input observed in these cells. Although decreased release probability has been associated with recent synaptic depression at the layer 4 to layer 2/3 synapse (Bender et al. 2006), these results suggest that excitatory drive onto fosGFP− cells is unlikely to have been reduced by some previously characterized plasticity mechanisms. Because the multiquantal response is larger but the single quantal response is the same, we conclude that fosGFP+ neurons receive more inputs from layer 4 neurons versus neighboring fosGFP− cells.

Consistent with this, analysis of EPSC amplitudes taken from the lowest stimulation intensities sampled showed that fosGFP− neurons showed an increased failure rate at low intensities (Supplementary Fig. S3; failure rate for paired recordings: fosGFP+ 0.25 ± 0.1 vs fosGFP− 0.72 ± 0.1, $n = 6$, $P < 0.05$). Taken together, these data suggest that fosGFP+ neurons receive a larger number of ascending inputs via layer 4 compared with fosGFP− cells.

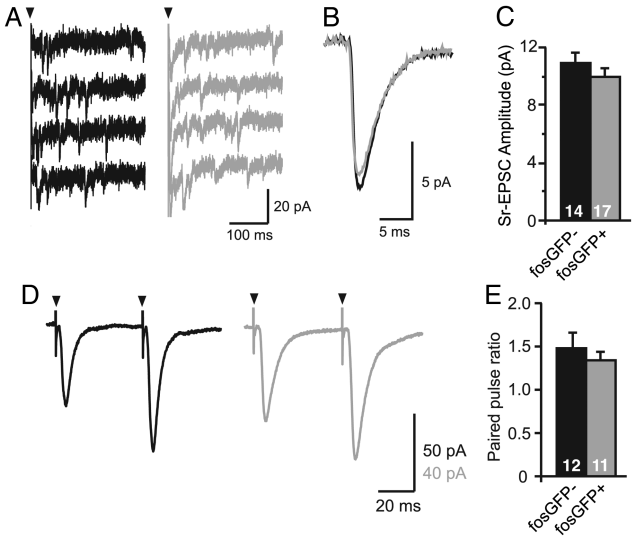

Figure 2. Properties of L4 to 2/3 excitatory synapses onto fosGFP+/− neurons. (*A*) L4-evoked miniature EPSCs (4 trials) recorded in a fosGFP− (black) or fosGFP+ (gray) L2/3 pyramidal cell in Sr-ACSF to desynchronize synaptic release. (*B*) Average Sr-EPSC recorded from all fosGFP− and all fosGFP+ neuron. (*C*) Mean ± SEM Sr-EPSC amplitude ($n = 17$ fosGFP+, $n = 14$ fosGFP−). (*D*) Example responses from fosGFP− (black) and fosGFP+ (gray) neurons to repetitive L4 stimulation (2 pulses, 20 Hz) used to calculate paired-pulse ratios. (*E*) Summary plot of mean ± SEM paired-pulse ratios for fosGFP− and fosGFP+ cells recorded at P11 to P14.

FosGFP+ Neurons Capture More Inputs During the Early Postnatal Period

Is this asymmetry in wiring established during early postnatal development? To determine whether fosGFP+ neurons show larger excitatory drive from layer 4 stimulation even at early stages of neocortical development, the amplitude of responses between fosGFP+ and fosGFP− cells was analyzed at P9–11, when the connection between layer 4 and layer 2/3 is first being established (Stern et al. 2001; Bender et al. 2003; Bureau et al. 2004). Although fosGFP expression was lower at this age, we were still able to find and record from pairs of fosGFP+ and fosGFP− cells (Fig. 3*A*). Layer 4-evoked EPSC amplitudes were not significantly different between the two populations of cells at this age (Fig. 3*B,C*; fosGFP+ 61.2 ± 6.9 pA vs fosGFP− 58.0 ± 7.4 pA, $n = 14$), indicating that IEG expression is not linked to input strength during early cortical development.

By P12, fosGFP+ neurons showed larger input strength (Fig. 3*D–F*, replotted from Fig. 1). Paired-cell recordings from older animals showed that this difference was diminished, on average, by the end of the third postnatal week (Fig. 3*G–I*; P18–22 fosGFP+ 57.2 ± 9.7 pA vs fosGFP− 50.2 ± 8.3 pA, $n = 9$), although EPSC amplitude was larger in fosGFP+ neurons in 7/9 cell pairs.

Asymmetric Wiring Requires Sensory Input to be Established but not Maintained

What events trigger and maintain the increased excitatory drive to this subset of layer 2/3 neurons? Is sensory input from the periphery required for fosGFP expression and the asymmetric wiring of layer 2/3 neurons? To test this, animals were deprived of whisker input beginning at P10 or P11 (Fig. 4*A*), and the difference in synaptic strength was compared between fosGFP+ and fosGFP− cells 24 h later. Notably, although sensory deprivation did not eliminate fosGFP expression in layer 2/3 neurons (Yassin et al. 2010), lack of whisker input for just one day during this critical time window was sufficient

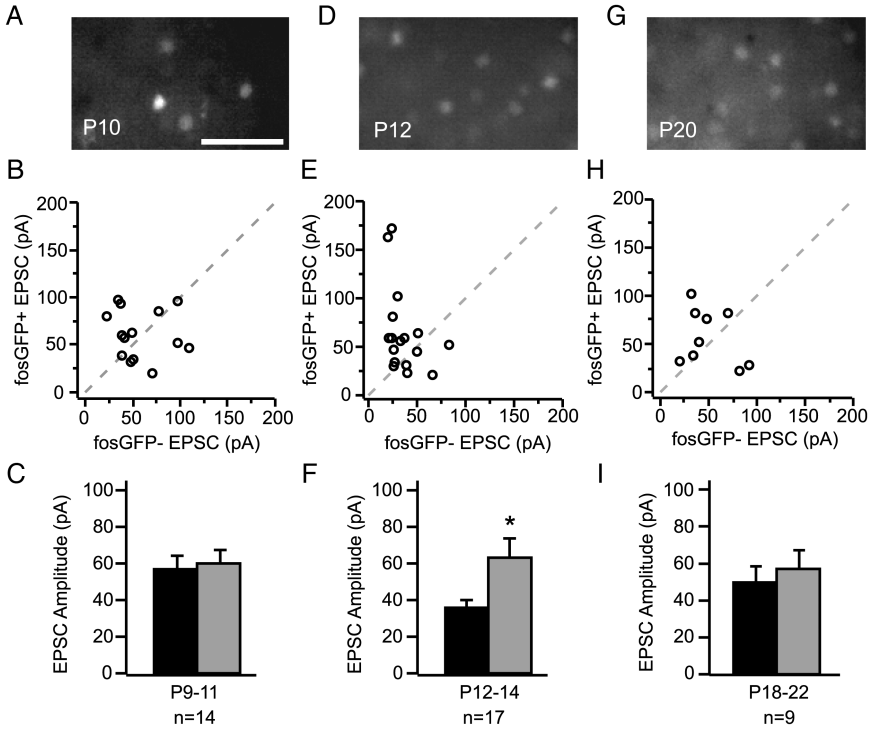

Figure 3. Excitation onto fosGFP+ and fosGFP− neurons is balanced in early development. (*A*) FosGFP expression in an acute brain slice from P10 mouse. Scale bar, 50 μm. (*B*) Scatter plot comparison of EPSC amplitudes recorded in fosGFP+/− pairs between P9 and P11. (*C*) Summary plot of average evoked EPSC amplitudes for the same cells as in (*B*). (*D–F*) FosGFP expression, scatter plot, and summary of EPSC amplitudes for fosGFP+/− pairs recorded between P12 and P14. Asterisk indicates $P < 0.05$. Data are replotted from Figure 1*D* and *F*. (*G–I*) FosGFP expression, scatter plot, and summary of EPSC amplitudes for fosGFP+/− pairs recorded between P18 and P22.

to abolish the difference in mean input strength between these two groups of cells (Fig. 4*B*,*D*; fosGFP+ 50.47 ± 8.8 pA vs fosGFP− 55.80 ± 8.5 pA, $n = 14$). In contrast, 24-h whisker deprivations that began later, in animals older than P12, had no effect on the 2-fold difference in evoked EPSC amplitude between these two cell groups (Fig. 4*C–D*; fosGFP+ 67.36 ± 6.8 pA vs fosGFP− 24.84 ± 0.8 pA, $n = 5$, $P < 0.05$). Therefore, sensory input is necessary to establish the stronger excitatory drive to fosGFP+ neurons from P9 to 11, but is not required for the maintenance of this difference in excitatory drive to layer 2/3 neurons.

FosGFP+ Neurons Fire at Lower Stimulus Thresholds Compared with fosGFP− Neurons

To test whether stronger excitatory drive is associated with lower stimulus intensity firing, dual-cell current-clamp recordings were carried out in fosGFP+ and fosGFP− neurons using an extracellular stimulating electrode in layer 4, where both excitation and inhibition remained intact in the slice (Fig. 5*A*, *B*). At low stimulus intensities, both fosGFP+ and fosGFP− cells exhibited a post-synaptic potential but no spike. As stimulus intensity was incrementally increased, fosGFP+ neurons began to fire at short latency (10–15 ms after the stimulus) on a fraction of trials, below the stimulus threshold for fosGFP− cells (Fig. 5*C*).

Does the reduced excitatory drive to fosGFP− cells mean that they can never fire with afferent stimulation? This was not observed to be the case. Both groups of cells exhibited a steep slope where firing reliability increased abruptly with increasing stimulus strength (Fig. 5*C*), until some point where both cells could be triggered to fire on every stimulus trial. Thus, increased stimulus strength can overcome the differences in excitatory drive between fosGFP+ and fosGFP− cells.

These findings were also replicated in paired juxta-cellular recordings (Fig. 5*D*; circles), indicating that differences in whole-cell recording conditions between the two cell types are unlikely to explain these results. Although the absolute value of the stimulus threshold required to generate a spike differed across different slice preparations, dual whole-cell recordings (Fig. 5*D*; triangles) revealed that overall fosGFP+ cells fired at significantly lower stimulus intensities compared with fosGFP− cells (Fig. 5*D*; $n = 13$ pairs, $P < 0.05$).

FosGFP+ Neurons Fire at Shorter Latencies

Because stimulus intensity and firing probability should be directly related to the timing of spikes in the post-synaptic cell, we hypothesized that fosGFP+ neurons might fire at shorter latencies than fosGFP− cells. Although stronger layer 4 stimulation intensities could drive both subsets of cell to fire reliably, fosGFP+ neurons fired significantly earlier at all stimulus intensity levels (Fig. 6*A*).

In order to compare response timing in pairs recorded from different slice preparations, we analyzed spike latency from stimulation intensities for which at least one cell in the recorded pair was firing on every trial. Here, fosGFP+ neurons responded significantly earlier than fosGFP− neighbors (Fig. 6*B*; fosGFP+ 9.73 ± 0.56 ms vs fosGFP− 12.44 ± 0.79 ms; $n = 20$; $P < 0.001$). Spikes in fosGFP+ neurons were also more precise (i.e. showed less trial-to-trial "jitter" of spike times) across multiple trials at a given stimulus intensity

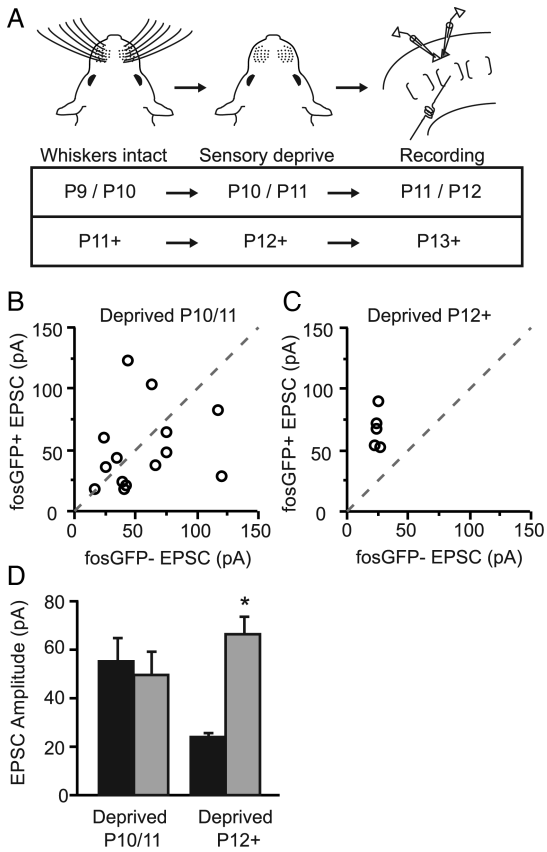

Figure 4. Asymmetric wiring requires sensory input to be established. (*A*) Experimental timelines used for sensory deprivation and brain slice recordings. (*B*) Scatter plot comparison of EPSC amplitudes recorded in fosGFP+/– pairs following 24 h of whisker deprivation initiated at P10/11. (*C*) Scatter plot comparison of EPSC amplitudes recorded in fosGFP+/– pairs following 24 h of whisker deprivation initiated after P11. (*D*) Summary histogram of evoked EPSC amplitudes from fosGFP +/– pairs (gray and black, respectively) following deprivation. Asterisk indicates $P < 0.05$.

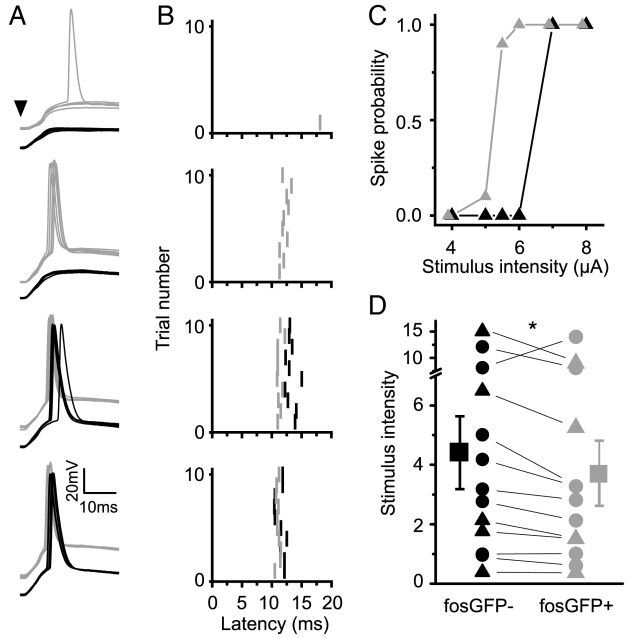

Figure 5. FosGFP+ cells fire more reliably to afferent stimulation. (*A*) Sample traces of whole-cell recordings in which responses evoked by L4 stimulation (at 4 different stimulation intensities 50, 60, 70, and 80 μA) were recorded in a pair of layer 2/3 fosGFP– (black) and fosGFP+ (gray) neurons. Arrowhead indicates stimulus onset. Stimulus artifacts have been truncated for clarity. (*B*) Raster plots of spike latencies showing the trial-by-trial responses of each neuron. Stimulus onset occurs at 0 ms. (*C*) Stimulus response curves of spiking probability for the example pair shown in A–B for six stimulation intensities. (*D*) Scatter plot of fosGFP+/– pairs (black triangles: whole-cell recordings; black circles: cell-attached recordings) where the value plotted on the *y*-axis is the extrapolated stimulus intensity corresponding to a 50% probability of neuronal firing. Asterisk indicates $P < 0.05$.

compared with fosGFP– cells (standard deviation of spike time fosGFP+ 0.54 ± 0.15 ms vs fosGFP– 0.93 ± 0.17 ms; $n = 14$ pairs).

Reduced Inhibition From Layer 4 Stimulation in fosGFP+ Neurons

Although the difference in excitatory drive between fosGFP+ and fosGFP– neurons was large, this increased excitatory drive might not be the only factor that facilitated lower stimulus-evoked firing. What other mechanisms could underlie this difference in stimulus-evoked firing between fosGFP+ and fosGFP– cells? Previous studies indicate that fosGFP+ neurons are not more excitable than fosGFP– cells, thus intrinsic electrophysiological properties are unlikely to explain the elevated firing output of fosGFP+ neurons (Yassin et al. 2010).

The strength of direct, monosynaptic inhibition resulting from layer 4 stimulation was evaluated by pharmacologically blocking recurrent excitation using the glutamate receptor antagonists NBQX and D-APV. Stimulus intensity was set so that both cells consistently showed a response (i.e., no failures), and the response amplitude ranged between 25 and 300 pA. These experiments did not reveal a significant difference in the amplitude of layer 4-evoked IPSCs between fosGFP+/– cells (Fig. 7*A*,*B*, fosGFP+ 87.77 ± 17.12 pA vs fosGFP– 103.39 ± 18.33 pA, $n = 11$). There was also no difference in the mean IPSC onset latency for these putatively monosynaptic events (Fig. 7*C*, fosGFP+ 5.04 ± 0.32 ms vs fosGFP– 4.74 ± 0.31 ms, $n = 11$). Thus, direct inhibition from layer 4 appears to be equivalent.

In order to examine whether there were differences in polysynaptic inhibition that might also result in spike suppression or delay in fosGFP– cells, IPSCs were electrically isolated by holding layer 2/3 neurons at +10 mV. Stimulus intensity was set so that a putative IPSC could be observed in both cells, where peak amplitude ranged from 25 to 300 pA. Responses typically showed multiple deflections in the fast rising phase of the response, indicative of a polysynaptic input. These dual whole-cell recordings revealed that fosGFP + cells received significantly less polysynaptic inhibition following layer 4 stimulation, compared with fosGFP– neurons (Fig. 7*D–F*, polysynaptic IPSC peak, fosGFP+ 91.6 ± 15 pA vs fosGFP– 152 ± 26 pA, $n = 12$ pairs, $P < 0.05$). Thus, differential inhibition may also contribute to firing output in these two groups of cells.

Discussion

In vivo imaging and recording studies have revealed that when activity is monitored in an unbiased manner, firing is sparsely distributed across populations of neocortical neurons in primary sensory cortex, even in awake animals (Brecht et al. 2003; de Kock et al. 2007; Crochet et al. 2011; but see

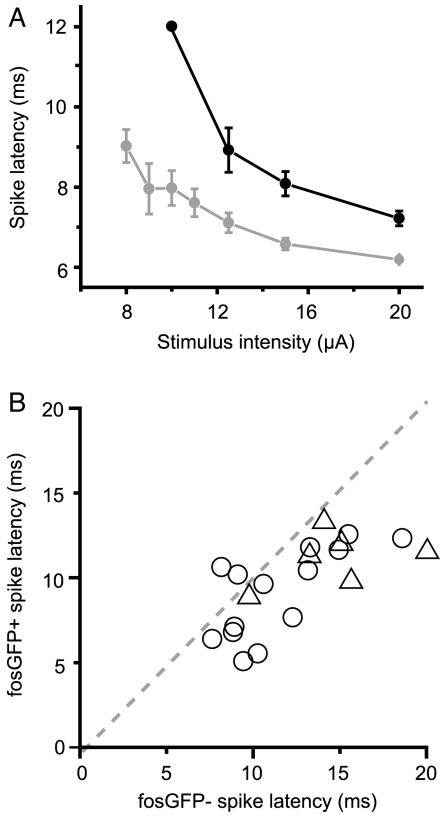

Figure 6. FosGFP+ neurons fire at shorter latency and with less jitter. (*A*) Spike latency at seven stimulation intensities for a single pair of fosGFP− (black) and fosGFP+ (gray) cells. Note that the standard deviation of spike times is reduced for the fosGFP+ cell. (*B*) Comparison of spike latencies for all fosGFP+/− pairs (Triangles: whole-cell recording; circles: juxta-cellular recording; values from stimulation intensities where at least one cell was firing on every stimulus trial; $n = 20$ pairs). Dashed line indicates unity.

Vijayan et al. 2010). The findings presented here indicate that a subset of pyramidal cells can fire at lower thresholds and more reliably than the majority of cells in the layer 2/3 network, and that this firing is due to increased excitatory and reduced inhibitory drive to these cells. These data indicate that short-latency, low-threshold firing in this subset of cells arises not from instantaneous variability in cortical state or noise, nor from the increased intrinsic excitability of fosGFP+ neurons, but rather through a difference in network wiring. The increased density of synaptic inputs through layer 4 to the highly active subnetwork of fosGFP-expressing neurons (Yassin et al. 2010) suggests that neocortical networks possess a hub-like architecture that may facilitate information propagation throughout the column.

Asymmetric Wiring in fosGFP+ and fosGFP− Neurons

How does this asymmetry in wiring arise? At very early developmental ages (P10–11), no difference in the amplitude of excitatory inputs elicited by layer 4 stimulation were observed. This abruptly changes at P12–13, a stage of cortical development where connections between layer 4 and layer 2/3 rapidly mature (Stern et al. 2001; Maravall et al. 2004; Wen and Barth 2011). This asymmetry requires sensory input to be established, since early whisker deprivation eliminated the difference in excitatory drive to fosGFP+ neurons. However, after this asymmetry arises, it was stable in the face of sensory deprivation, since later deprivation (at P13, for example) did not normalize synaptic strength between the two groups of cells. The maturation of neocortical circuits continues to progress during the third and fourth postnatal week (Feldmeyer et al. 2002; Feldmeyer et al. 2006). Dual-cell recordings from older animals indicated a trend for fosGFP+ neurons to show stronger excitatory drive at the close of the third postnatal week as well, though this difference was no

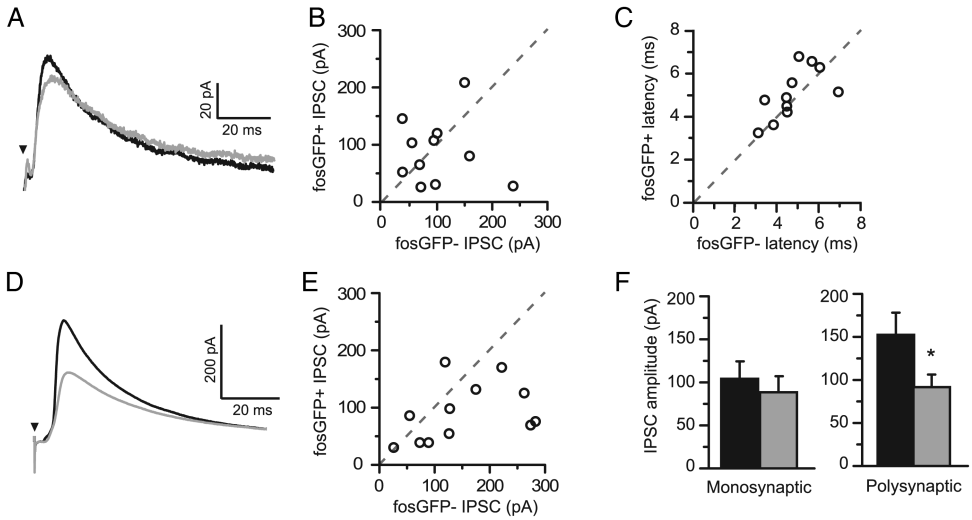

Figure 7. FosGFP+ cells receive less synaptic inhibition. (*A*) Average sample traces of monosynaptic inhibitory post-synaptic currents (IPSCs) evoked by L4 stimulation in the presence of APV and NBQX recorded simultaneously in a pair of fosGFP+/− neurons (gray and black, respectively). (*B*) Scatter plot comparison of monosynaptic IPSC amplitudes for 11 fosGFP+/− pairs. (*C*) Scatter plot comparison of IPSC onset latency for the same pairs as in B. (*D*) Average sample traces of polysynaptic IPSCs evoked by L4 stimulation recorded in a fosGFP+/− pairs voltage clamped to the experimentally determined EPSC reversal potential (+10 mV) in the absence of any drugs to block excitatory synaptic transmission. (*E*) Scatter plot comparison of polysynaptic IPSC amplitudes for 12 fosGFP+/− pairs. (*F*) Summary histograms of mono- (left) and polysynaptic (right) IPSC amplitudes. Asterisk indicates $P < 0.05$.

longer statistically significant. Future experiments will be required to address the stability of this network in older animals.

Sources of Differential Input to Layer 2/3 Neurons

The extracellular stimulation paradigm employed here did not isolate layer 4 afferents from other inputs, such as thalamocortical or infragranular inputs that ascend to layer 3. Although the most dense source of input to layer 3 comes from spiny stellate cells in layer 4 (Feldmeyer et al. 2002), other investigators have noted that some thalamic inputs target layer 3 and layer 2 (Meyer et al. 2010), and that layer 5 shows weak connectivity to layer 3 (Lefort et al. 2009; Oberlaender et al. 2011). In addition, axons from other cortical areas (i.e., the contralateral hemisphere; Aronoff et al. 2010) may ascend through the barrel. Thus, it is possible that the differential synaptic drive observed in these two groups of cells may arise from other sources besides layer 4. Although layer 4 to layer 2/3 connections appear to be present as early as P10 (Bender et al. 2003; Bureau et al. 2004) they undergo substantial refinement in subsequent days (Bender et al. 2003), and sensory–response properties are not detectable at this time (Stern et al. 2001; Benedetti et al. 2009). The developmental regulation of inputs from other cortical layers has not been well studied, but may be relevant in understanding the asymmetry in synaptic drive described here.

It is also possible that different subsets of layer 4 neurons target their projections to layer 3 neurons (for example, Yoshimura et al. 2005). Although technically challenging, it will be of interest to determine whether inputs from a single layer 4 neuron converge onto both fosGFP+ and fosGFP− neurons, and whether this changes during development. These data may help evaluate the hypothesis that competitive processes (vs molecularly specified connectivity) drive the wiring of neocortical circuits.

Sensory Deprivation and fosGFP Expression

What maintains fosGFP expression during sensory deprivation? This is an interesting question, since stronger synaptic input from layer 4 might be the primary source of increased activity that drives fosGFP expression. However, our previous work showed that fosGFP+ neurons also show greater connectivity to each other within layer 2/3 (Yassin et al. 2010), suggesting that there may also be intralaminar networks that drive firing and IEG expression, independently of sensory input. We note that the specific stimulus that drives fosGFP expression in a given cell is not easy to determine, since it occurred in vivo, during normal behavior. Thus, our results simply correlate a well-accepted marker of neuronal activity with specific wiring differences between layer 4 and layer 2/3 in the cortical network.

Hallmarks of Plasticity in More Active Neurons are Absent

Although experience-dependent plasticity has been well characterized at layer 4 to layer 2/3 inputs, we found no evidence for recent synaptic potentiation—such as an increase in the quantal amplitude of Sr-evoked EPSCs—in fosGFP+ neurons that might explain their stronger excitatory drive. This is surprising, since the post-synaptic addition of glutamate receptors is a well-characterized mechanism for synaptic strengthening at layer 4 to layer 2/3 synapses during this developmental time period (Clem and Barth 2006; Clem et al. 2008; Wen and Barth 2011). Furthermore, most models of activity-dependent synaptic plasticity predict that more active neurons should accumulate larger inputs via potentiation of existing inputs (Markram et al. 1997; Bi and Poo 1998). Instead, the increased number of inputs may be a developmentally specified and persistent feature of this cell population.

Conversely, we found no evidence for synaptic depression in fosGFP− neurons—such as an increase in the PPR which has been characterized following experience-dependent plasticity at the layer 4 to layer 2/3 synapses in S1 (Bender et al. 2006). Although we cannot rule out other types of synaptic strengthening that might not be apparent by these traditional measures, our data are more consistent with a model by which fosGFP+ neurons recruit a greater number of inputs during construction of the layer 4 to layer 2/3 circuit in the second postnatal week.

During development in many systems, axonal inputs grow exuberantly into their target region and then are pruned by patterned activity by well-characterized synaptic plasticity mechanisms (reviewed by Waites et al. 2005). If input strength between fosGFP+ and fosGFP− neurons is similar at the earliest stages of axonal connectivity from layer 4 to layer 2/3, asymmetric wiring might also be accomplished by selective synaptic removal to fosGFP− neurons, although this is typically associated with synaptic depression. Alternatively, molecular cues might direct the construction of specific circuits during the development of these inputs in the absence of direct plasticity.

Difference in Spike Timing Between fosGFP+ and fosGFP− Neurons

One implication of the current study is that fosGFP+ neurons may fire more synchronously during activation of the cortical column. This ensemble may be effective at driving specific downstream neurons in the cortex, propagating information transfer across multiple synapses (Salinas and Sejnowski 2001; Reyes 2003; Kumar et al. 2010). Based upon the findings presented here, spiking of fosGFP+ neurons may differentially represent low-intensity stimuli, but it is also possible that they encode a separate stream of unidentified sensory information.

The reduced jitter of the spike output in fosGFP+ neurons may be important for spike-timing dependent plasticity, where in vitro analyses show that the specific time interval between the post-synaptic EPSC and spike over multiple stimulus presentations may be critical for encoding the sign of synaptic change (Bi and Poo 1998). However, the lack of evidence for recent synaptic plasticity at putative layer 4 to layer 2/3 inputs suggests that under basal (home cage, resting) conditions, spike-timing dependent mechanisms are not differentially reconfiguring synaptic strength at fosGFP+ and fosGFP− cells.

The small but significant difference in spike timing may also facilitate the separation of this stream of information across later synapses. Studies in other systems have established that at least in some neocortical areas, millisecond timescale differences in firing can be behaviorally reported (Yang et al. 2008). The difference in firing between fosGFP+ and fosGFP− neurons may thus retain stimulus information that is

available for perception and decision making. Although sufficiently strong layer 4 extracellular stimulation could drive both fosGFP+ and fosGFP− neurons to fire, we note that this intensity may not be physiologically relevant. Future experiments using in vivo stimulation and recording will be required to determine whether these differences are relevant in the awake and behaving animal.

Functional Subcircuits of Layer 2/3 Neurons

Previous studies indicate that both the frequency and amplitude of miniature EPSCs and IPSCs, measured under conditions where neuronal firing in the slice is blocked using the sodium channel antagonist TTX, are identical between fosGFP+ and fosGFP− neurons (Yassin et al. 2010). Thus, if fosGFP+ neurons receive a greater number of inputs from layer 4, this must be balanced by a reduced number of inputs from some other source. Although the source of other inputs that differentially wire to fosGFP+ and fosGFP− neurons remains unknown, these data are consistent with the possibility that these two cell types may participate in different cortical subcircuits. Although the presence of interdigitated cortical subcircuits has been described in other neocortical layers (specifically, layer 5; Song et al. 2005; Perin et al. 2011), this phenomenon has not been well characterized in layer 2/3.

Previous studies, including ones from our laboratory, have suggested that there are other embedded subnetworks of neocortical neurons—both inhibitory and excitatory—that may be molecularly defined (Hestrin and Galarreta 2005; Yoshimura et al. 2005; Brown and Hestrin 2009; Yassin et al. 2010; Otsuka and Kawaguchi 2011). However, the function of these subnetworks, especially with regard to what they may encode, has not been determined. Understanding the response properties and information transformations that occur in different cortical subcircuits is a major goal in contemporary neuroscience.

Conclusion

The data presented here show that response heterogeneity in the cortex can be determined by significant differences in both excitatory and inhibitory circuit properties that are established by the second and third postnatal weeks. These studies suggest that specific groups of layer 2/3 neurons, marked by activity history and IEG expression, may more robustly respond to peripheral stimulation. Identification of a cell subpopulation with differential firing output will facilitate analysis into the cellular and molecular mechanisms that are critical for sparse encoding of sensory information in neocortical circuits.

Supplementary Material

Supplementary material can be found at: http://www.cercor.oxfordjournals.org/.

Funding

This work was supported by National Institutes of Health (DA017188).

Notes

We thank Joanne Steinmiller for expert animal care, and Rick Gerkin for data acquisition and analysis support for IGOR Pro. We are grateful to Rick Gerkin, Brent Doiron, and Nathan Urban for helpful comments on the manuscript in its early stages. *Author contributions*: A.L.B, B.L.B., Y.T., and J.A.W. conceived the study, designed the experiments, and co-wrote the manuscript. B.L.B., Y.T., J.A.W., and J.U.C. carried out the experiments. All the authors read and approved the manuscript. *Conflict of Interest*: A patent is pending on the fosGFP transgenic mice (A.L.B.).

References

Arieli A, Sterkin A, Grinvald A, Aertsen A. 1996. Dynamics of ongoing activity: explanation of the large variability in evoked cortical responses. Science (New York, NY). 273:1868–1871.

Aronoff R, Matyas F, Mateo C, Ciron C, Schneider B, Petersen CC. 2010. Long-range connectivity of mouse primary somatosensory barrel cortex. Eur J Neurosci. 31:2221–2233.

Barth AL, Gerkin RC, Dean KL. 2004. Alteration of neuronal firing properties after in vivo experience in a FosGFP transgenic mouse. J Neurosci. 24:6466–6475.

Barth AL, Poulet JF. 2012. Experimental evidence for sparse firing in the neocortex. Trends Neurosci. 35:345–355.

Bender KJ, Allen CB, Bender VA, Feldman DE. 2006. Synaptic basis for whisker deprivation-induced synaptic depression in rat somatosensory cortex. J Neurosci. 26:4155–4165.

Bender KJ, Rangel J, Feldman DE. 2003. Development of columnar topography in the excitatory layer 4 to layer 2/3 projection in rat barrel cortex. J Neurosci. 23:8759–8770.

Benedetti BL, Glazewski S, Barth AL. 2009. Reliable and precise neuronal firing during sensory plasticity in superficial layers of primary somatosensory cortex. J Neurosci. 29:11817–11827.

Bi GQ, Poo MM. 1998. Synaptic modifications in cultured hippocampal neurons: dependence on spike timing, synaptic strength, and postsynaptic cell type. J Neurosci. 18:10464–10472.

Brecht M, Roth A, Sakmann B. 2003. Dynamic receptive fields of reconstructed pyramidal cells in layers 3 and 2 of rat somatosensory barrel cortex. J Physiol. 553:243–265.

Brown SP, Hestrin S. 2009. Cell-type identity: a key to unlocking the function of neocortical circuits. Curr Opin Neurobiol. 19:415–421.

Bureau I, Shepherd GM, Svoboda K. 2004. Precise development of functional and anatomical columns in the neocortex. Neuron. 42:789–801.

Clem RL, Barth A. 2006. Pathway-specific trafficking of native AMPARs by in vivo experience. Neuron. 49:663–670.

Clem RL, Celikel T, Barth AL. 2008. Ongoing in vivo experience triggers synaptic metaplasticity in the neocortex. Science (New York, NY). 319:101–104.

Constantinople CM, Bruno RM. 2011. Effects and mechanisms of wakefulness on local cortical networks. Neuron. 69:1061–1068.

Crochet S, Poulet JFA, Kremer Y, Petersen CH. 2011. Synaptic mechanisms underlying sparse coding of active touch. Neuron. 69:1–16.

de Kock CP, Bruno RM, Spors H, Sakmann B. 2007. Layer- and cell-type-specific suprathreshold stimulus representation in rat primary somatosensory cortex. J Physiol. 581:139–154.

Feldmeyer D, Lubke J, Sakmann B. 2006. Efficacy and connectivity of intracolumnar pairs of layer 2/3 pyramidal cells in the barrel cortex of juvenile rats. J Physiol. 575:583–602.

Feldmeyer D, Lubke J, Silver RA, Sakmann B. 2002. Synaptic connections between layer 4 spiny neurone-layer 2/3 pyramidal cell pairs in juvenile rat barrel cortex: physiology and anatomy of interlaminar signalling within a cortical column. J Physiol. 538:803–822.

Fields RD, Eshete F, Stevens B, Itoh K. 1997. Action potential-dependent regulation of gene expression: temporal specificity in ca2+, cAMP-responsive element binding proteins, and mitogen-activated protein kinase signaling. J Neurosci. 17:7252–7266.

Goda Y, Stevens CF. 1994. Two components of transmitter release at a central synapse. Proc Natl Acad Sci USA. 91:12942–12946.

Guzowski JF, Miyashita T, Chawla MK, Sanderson J, Maes LI, Houston FP, Lipa P, McNaughton BL, Worley PF, Barnes CA. 2006. Recent

behavioral history modifies coupling between cell activity and Arc gene transcription in hippocampal CA1 neurons. Proc Natl Acad Sci USA. 103:1077–1082.
Hestrin S, Galarreta M. 2005. Electrical synapses define networks of neocortical GABAergic neurons. Trends Neurosci. 28:304–309.
Hromadka T, Deweese MR, Zador AM. 2008. Sparse representation of sounds in the unanesthetized auditory cortex. PLoS Biol. 6:e16.
Kenet T, Bibitchkov D, Tsodyks M, Grinvald A, Arieli A. 2003. Spontaneously emerging cortical representations of visual attributes. Nature. 425:954–956.
Kerr JN, de Kock CP, Greenberg DS, Bruno RM, Sakmann B, Helmchen F. 2007. Spatial organization of neuronal population responses in layer 2/3 of rat barrel cortex. J Neurosci. 27:13316–13328.
Kumar A, Rotter S, Aertsen A. 2010. Spiking activity propagation in neuronal networks: reconciling different perspectives on neural coding. Nat Rev Neurosci. 11:615–627.
Lefort S, Tomm C, Floyd Sarria JC, Petersen CC. 2009. The excitatory neuronal network of the C2 barrel column in mouse primary somatosensory cortex. Neuron. 61:301–316.
Luckman SM, Dyball RE, Leng G. 1994. Induction of c-fos expression in hypothalamic magnocellular neurons requires synaptic activation and not simply increased spike activity. J Neurosci. 14:4825–4830.
MacLean JN, Watson BO, Aaron GB, Yuste R. 2005. Internal dynamics determine the cortical response to thalamic stimulation. Neuron. 48:811–823.
Maravall M, Stern EA, Svoboda K. 2004. Development of intrinsic properties and excitability of layer 2/3 pyramidal neurons during a critical period for sensory maps in rat barrel cortex. J Neurophysiol. 92:144–156.
Marder E, Goaillard JM. 2006. Variability, compensation and homeostasis in neuron and network function. Nat Rev Neurosci. 7:563–574.
Markram H, Lubke J, Frotscher M, Sakmann B. 1997. Regulation of synaptic efficacy by coincidence of postsynaptic APs and EPSPs. Science (New York, NY). 275:213–215.
Marre O, Yger P, Davison AP, Fregnac Y. 2009. Reliable recall of spontaneous activity patterns in cortical networks. J Neurosci. 29:14596–14606.
Metherate R, Cox CL, Ashe JH. 1992. Cellular bases of neocortical activation: modulation of neural oscillations by the nucleus basalis and endogenous acetylcholine. J Neurosci. 12:4701–4711.
Meyer HS, Wimmer VC, Hemberger M, Bruno RM, de Kock CP, Frick A, Sakmann B, Helmstaedter M. 2010. Cell type-specific thalamic innervation in a column of rat vibrissal cortex. Cereb Cortex. 20:2287–2303.
Oberlaender M, Boudewijns ZS, Kleele T, Mansvelder HD, Sakmann B, de Kock CP. 2011. Three-dimensional axon morphologies of individual layer 5 neurons indicate cell type-specific intracortical pathways for whisker motion and touch. Proc Natl Acad Sci USA. 108:4188–4193.
Ohki K, Chung S, Ch'ng YH, Kara P, Reid RC. 2005. Functional imaging with cellular resolution reveals precise micro-architecture in visual cortex. Nature. 433:597–603.
Otsuka T, Kawaguchi Y. 2011. Cell diversity and connection specificity between callosal projection neurons in the frontal cortex. J Neurosci. 31:3862–3870.
Padmanabhan K, Urban NN. 2010. Intrinsic biophysical diversity decorrelates neuronal firing while increasing information content. Nat Neurosci. 13:1276–1282.
Perin R, Berger TK, Markram H. 2011. A synaptic organizing principle for cortical neuronal groups. Proc Natl Acad Sci USA. 108:5419–5424.
Petersen CC, Hahn TT, Mehta M, Grinvald A, Sakmann B. 2003. Interaction of sensory responses with spontaneous depolarization in layer 2/3 barrel cortex. Proc Natl Acad Sci USA. 100:13638–13643.
Poo C, Isaacson JS. 2009. Odor representations in olfactory cortex: "sparse" coding, global inhibition, and oscillations. Neuron. 62:850–861.
Reyes AD. 2003. Synchrony-dependent propagation of firing rate in iteratively constructed networks in vitro. Nat Neurosci. 6:593–599.
Salinas E, Sejnowski TJ. 2001. Correlated neuronal activity and the flow of neural information. Nat Rev Neurosci. 2:539–550.
Schilling K, Luk D, Morgan JI, Curran T. 1991. Regulation of a fos-lacZ fusion gene: a paradigm for quantitative analysis of stimulus-transcription coupling. Proc Natl Acad Sci USA. 88:5665–5669.
Schoenenberger P, Gerosa D, Oertner TG. 2009. Temporal control of immediate early gene induction by light. PloS One. 4:e8185.
Sheng M, McFadden G, Greenberg ME. 1990. Membrane depolarization and calcium induce c-fos transcription via phosphorylation of transcription factor CREB. Neuron. 4:571–582.
Song S, Sjostrom PJ, Reigl M, Nelson S, Chklovskii DB. 2005. Highly nonrandom features of synaptic connectivity in local cortical circuits. PLoS Biol. 3:e68.
Steriade M, Amzica F, Nunez A. 1993. Cholinergic and noradrenergic modulation of the slow (approximately 0.3 Hz) oscillation in neocortical cells. J Neurophysiol. 70:1385–1400.
Stern EA, Maravall M, Svoboda K. 2001. Rapid development and plasticity of layer 2/3 maps in rat barrel cortex in vivo. Neuron. 31:305–315.
Stettler DD, Axel R. 2009. Representations of odor in the piriform cortex. Neuron. 63:854–864.
Thomas MJ, Beurrier C, Bonci A, Malenka RC. 2001. Long-term depression in the nucleus accumbens: a neural correlate of behavioral sensitization to cocaine. Nat Neurosci. 4:1217–1223.
Vijayan S, Hale GJ, Moore CI, Brown EN, Wilson M. 2010. Activity in the barrel cortex during active behavior and sleep. J Neurophysiol. 103:2074–2084.
Waites CL, Craig AM, Garner CC. 2005. Mechanisms of vertebrate synaptogenesis. Annu Rev Neurosci. 28:251–274.
Wen JA, Barth AL. 2011. Input-specific critical periods for experience-dependent plasticity in layer 2/3 pyramidal neurons. J Neurosci. 31:4456–4465.
Wolfe J, Houweling AR, Brecht M. 2010. Sparse and powerful cortical spikes. Curr Opin Neurobiol. 20:306–312.
Xu-Friedman MA, Regehr WG. 1999. Presynaptic strontium dynamics and synaptic transmission. Biophys J. 76:2029–2042.
Yang Y, DeWeese MR, Otazu GH, Zador AM. 2008. Millisecond-scale differences in neural activity in auditory cortex can drive decisions. Nat Neurosci. 11:1262–1263.
Yassin L, Benedetti BL, Jouhanneau JS, Wen JA, Poulet JFA, Barth AL. 2010. An embedded subnetwork of highly active neurons in the neocortex. Neuron. 68:1043–1050.
Yoshimura Y, Dantzker JL, Callaway EM. 2005. Excitatory cortical neurons form fine-scale functional networks. Nature. 433:868–873.